

$^{209}\text{Bi}(^6\text{He}, \alpha)$ reaction mechanisms studied near the Coulomb barrier using n– α coincidence measurements

J.P. Bychowski^{a,1}, P.A. DeYoung^{a,*}, B.B. Hilldore^a, J.D. Hinnefeld^b, A. Vida^b,
F.D. Becchetti^c, J. Lupton^c, T.W. O'Donnell^c, J.J. Kolata^d, G. Rogachev^d,
M. Hencheck^e

^a Department of Physics and Engineering Hope College, Holland, MI 49422-9000, USA

^b Physics Department, Indiana University South Bend, South Bend, IN 46634-7111, USA

^c Physics Department, University of Michigan, Ann Arbor, MI 48109-1120, USA

^d Physics Department, University of Notre Dame, Notre Dame, IN 46556-5670, USA

^e Department of Natural and Applied Sciences, University of Wisconsin-Green Bay, Green Bay, WI 54311, USA

Received 24 March 2004; received in revised form 5 May 2004; accepted 6 May 2004

Available online 22 June 2004

Editor: J.P. Schiffer

Abstract

The $^6\text{He} + ^{209}\text{Bi}$ reaction displays a remarkably large cross section for α -particle emission at energies near the Coulomb barrier. The possible reactions that may produce the observed α particles include two-neutron transfer, one-neutron transfer, and direct projectile breakup. Each of these mechanisms results in a distinctive angular correlation between the α particle and outgoing neutron(s). A neutron- α -particle coincidence experiment was performed to separate these different modes. The neutron data show significant angular correlations. Monte Carlo simulations of one-neutron transfer are compared with the experimental data. It is shown that approximately 20% of the observed α -particle yield is due to this process.

© 2004 Elsevier B.V. Open access under [CC BY license](https://creativecommons.org/licenses/by/4.0/).

PACS: 25.60.-t; 25.60.Je; 27.20.+n

Keywords: ^6He ; Transfer reaction; Breakup reaction; Neutron- α particle coincidence

1. Introduction

The radioactive nucleus ^6He has been widely studied because its neutron halo greatly affects the manner in which it interacts with other nuclei. Measurements have been made of evaporation products after the fusion of ^6He with ^{209}Bi [1–3], as well as the spin distribution in the compound system [4]. The proba-

* Corresponding author.

E-mail addresses: deyoung@hope.edu (P.A. DeYoung), fdb@umich.edu (F.D. Becchetti), james.j.kolata.1@nd.edu (J.J. Kolata).

¹ Physics Department, University of Notre Dame, Notre Dame, IN 46556-5670, USA.

bility of fission after the fusion of ${}^6\text{He}$ with ${}^{209}\text{Bi}$ and ${}^{238}\text{U}$ has also been determined [3,5–7]. The conclusion from these experiments was that the sub-barrier fusion of ${}^6\text{He}$ with high- Z targets is significantly enhanced. In another investigation [8] of ${}^6\text{He} + {}^{209}\text{Bi}$ reactions at energies near the Coulomb barrier, especially large yields of α particles were observed. Most recently, similar strong α yields were seen in a measurement of ${}^6\text{He}$ with ${}^{64}\text{Zn}$ [9] but without the fusion enhancement reported elsewhere. The angular distribution of Ref. [8] was characteristic of a direct reaction, and the total cross section for the emission of an α particle was reported to be 773 mb at 22.5 MeV and 643 mb at 19 MeV laboratory ${}^6\text{He}$ energy. In comparison, the fusion cross sections at these energies are 310 ± 45 mb and 75 ± 17 mb, respectively [2]. Unfortunately, the reaction mechanisms responsible for these large α -particle yields cannot be determined from the existing data. It has been suggested that one- and two-neutron transfer processes might play a decisive role because preliminary calculations [8] indicate that neutron transfer can be significantly enhanced by coupling to continuum states in reactions of weakly-bound nuclei such as ${}^6\text{He}$. Furthermore, enhanced neutron transfer also appears to drive an enhancement in the fusion yield [8]. The goal of the present experiment was to achieve a better understanding of the mechanisms responsible for the large α -particle cross sections reported in the previous work. There are three possible mechanisms that could yield an α particle: two-neutron transfer followed by evaporation, one-neutron transfer followed by ${}^5\text{He}$ breakup, and direct projectile breakup. Intuitively, each of these reactions has a distinctive neutron angular distribution relative to the direction of the emitted α particle.

2. Experimental detail

The experiment was carried out at the Nuclear Structure Laboratory of the University of Notre Dame. A primary beam of ${}^7\text{Li}$ at a laboratory energy of 29 MeV was incident on a ${}^9\text{Be}$ production target. The TWINSOL [10] radioactive nuclear beam facility was used to focus the resulting ${}^6\text{He}$ beam into a secondary target chamber located in a shielded room 7.5 m downstream of the primary target, while rejecting unwanted secondary beam species. In order to reduce the intense neutron and γ -ray background coming from the pri-

mary target, TWINSOL was used in the “no-crossover” mode and 60 cm of high-density polyethylene followed by 30 cm of ‘Heavymet’ shielding was introduced on the beam axis between the primary and secondary targets. Furthermore, a wall of water containing dissolved borax (sodium tetraborate pentahydrate) was situated at the entrance to the room containing the secondary target chamber. See Ref. [11] for more discussion of the neutron and γ -ray shielding.

The ${}^{209}\text{Bi}$ target had an areal density of 3.25 mg/cm², and the laboratory energy of the ${}^6\text{He}$ beam at the center of the target was 22.9 MeV. This is just above the Coulomb barrier, which is at approximately 20 MeV [8]. The α particles were detected in two Si ΔE – E telescopes mounted at angles of -90° and 120° relative to the beam axis. Since the telescopes were only 4 cm from the target and the beam was approximately 8 mm in diameter, a Monte Carlo simulation was carried out to determine their effective solid angle. The solid angles of the -90° and 120° telescopes were found to be 217 ± 0.4 msr and 213 ± 0.4 msr, respectively. The solid angles were found to be insensitive to the beam spot size and the quoted errors are based on the statistics of the simulation. The ΔE – E telescopes provided particle identification, an example of which can be seen in Fig. 1. It is evident that the different nuclear species form well-defined and readily identifiable groups. The α -particle direct beam contaminants are off the scale of Fig. 1 to the right and cannot be mistaken for reaction products. The projection of the α events onto the energy axis

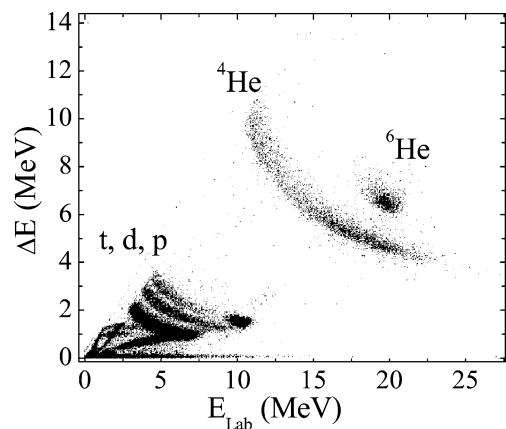


Fig. 1. Typical ΔE – E spectrum, taken at $\Theta_{\text{lab}} = 135^\circ$ and ${}^6\text{He}$ beam energy $E_{\text{lab}} = 22.9$ MeV.

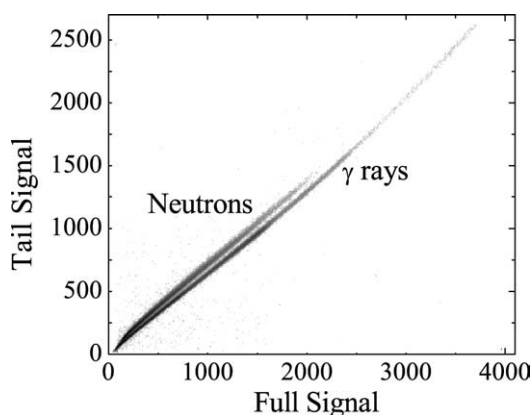


Fig. 2. Typical n - γ separation for the neutron detector at $\Theta_{\text{lab}} = -90^\circ$, obtained with a PuBe source.

is identical in shape to that shown in Fig. 1 of Ref. [8]. The signal from the α -particle detector also served as the event trigger for the neutron coincidence and time-of-flight measurement.

The inclusive α -particle cross sections at -90° and 120° were measured in the present experiment to be 62 mb/sr and 41 mb/sr, respectively. The uncertainties, dominated by systematic error, are estimated to be approximately $\pm 25\%$ since the data were normalized to the primary beam current (see Ref. [8] for a discussion of this procedure) rather than to Rutherford scattering. These cross sections are somewhat lower than, but consistent with, the 80 and 66 mb/sr reported in Ref. [8]. Thus, the α -particle data from the present measurement confirm the large yields previously reported.

Eight 12.7 cm diameter by 5 cm deep NE213 liquid scintillator detectors were used to detect the neutrons. They were placed in the reaction plane, and at angles of -90° , -69.5° , -54° , -15° , 30° , 60° , 101° , and 120° relative to the beam axis. Pulse-shape discrimination was used to separate neutrons from γ rays. Fig. 2 shows a typical neutron/ γ -ray discrimination spectrum for one of the detectors. The detection threshold was approximately 150–200 keV electron equivalent energy for each detector, as determined with γ -ray sources.

3. Results and interpretation

The angular distribution of neutrons in coincidence with α particles is shown in Fig. 3. The neutron yield

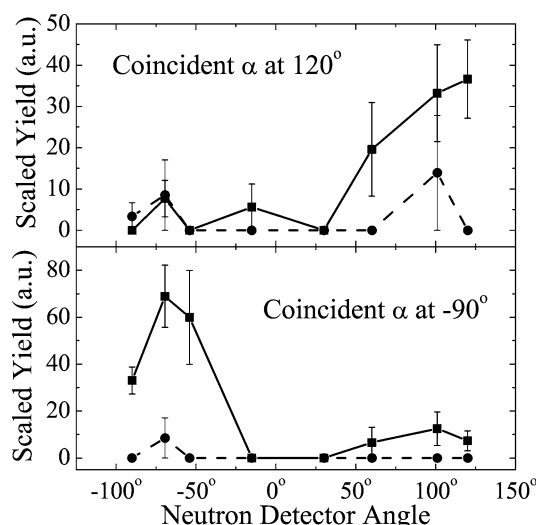


Fig. 3. The observed number of neutrons coincident with α particles, displayed vs. neutron detection angle. The square points are the ^{209}Bi -target data. The circular points are the mylar-backing data. Lines have been placed on the graph to guide the eye.

for each of the liquid scintillator detectors was scaled by normalizing to the solid angle of the -90° neutron detector (0.148 sr). The error bars are based only on counting statistics. It is apparent from Fig. 3 that there is a strong correlation between the emission angles of the α -particles and the coincident neutrons. Also shown in Fig. 3 are the neutron yields from a mylar target (the same material used as the backing for the ^{209}Bi target). The mylar data have been multiplied by an additional scaling factor to compensate for the different amounts of beam current that each target experienced during the experiment. The neutron yield from the mylar target is consistent with zero at all angles.

The physics involved in the reaction mechanism determines the angular distribution of coincident neutrons for each of three postulated reactions: two-neutron transfer, one-neutron transfer, and direct projectile breakup. For two-neutron transfer we consider that, as the ^6He scatters from the ^{209}Bi , the two valence neutrons are transferred forming ^{211}Bi . Later, one or two neutrons may be evaporated from this compound system. In this case there would be little or no correlation between the α -particle and neutron emission angles. For one-neutron transfer, a single neutron is transferred to ^{209}Bi leaving an unstable ^5He which im-

mediately breaks up. After breakup occurs, the center-of-momentum of the α particle and the neutron continues on the same path as the ${}^5\text{He}$, perturbed only by the breakup energy. The neutron and the α particle would have a strong angular correlation. In the case of direct projectile breakup, the ${}^6\text{He}$ is assumed to fragment into an α particle and two neutrons near the distance of closest approach. The neutrons then follow the velocity vector of the ${}^6\text{He}$ at the instant of breakup while the α -particle continues under the influence of the Coulomb force. This process results in a neutron distribution that is focused at more forward angles than the α -particle distribution.

A Monte Carlo simulation was carried out for one-neutron transfer in an attempt to quantitatively determine the contribution of this reaction mechanism. The assumption was made that the ${}^5\text{He}$ reaction products would have the same mean energy-per-nucleon and azimuthal angular distribution as the α particles reported in Ref. [8]. The detector geometry and beam profile were included in the simulation. After the emission properties were chosen, the ${}^5\text{He}$ was allowed to break up, isotropically in its rest frame, with a decay energy of 890 keV. The intersection of the α -particle trajectory with the plane of the Si ΔE – E telescopes, as well as the intersection of the neutron trajectory with the plane of the liquid-scintillator detectors, were calculated. If the intersections of the particles with the detector planes occurred within the radius of the detectors, the particle was assumed to be detected. The coincident neutrons in the simulation were normalized by scaling the number of simulated α particles that hit the ΔE – E telescopes to the total number of α particles detected in the experiment, without taking neutron coincidence into account. In addition, an average efficiency of 30% for the neutron detectors at the energies observed was incorporated into this normalization. In this way, the predicted yield of neutrons in the simulation is equivalent to that which would be observed if all the α particles resulted from one-neutron transfer. Fig. 4 shows the normalized angular distribution of coincident neutrons from simulated one-neutron transfer.

A projectile-breakup simulation was also attempted by selecting ${}^6\text{He}$ during Rutherford scattering according to a random impact parameter uniformly distributed about the beam axis. It was assumed that the ${}^6\text{He}$ fragmented into two neutrons and an α particle at

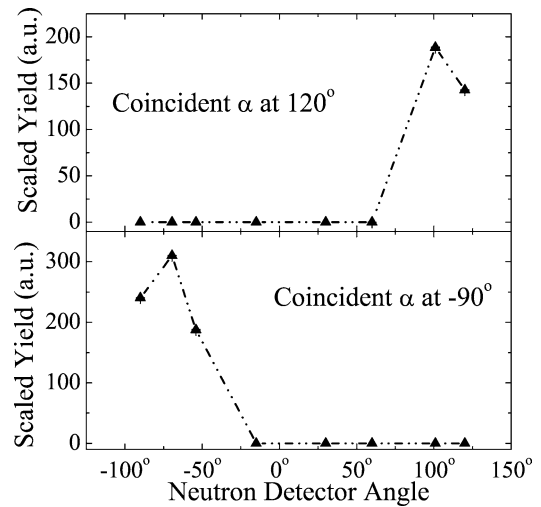


Fig. 4. The number of neutrons coincident with α particles, from the one-neutron-transfer Monte Carlo simulation under the assumption that the entire α -particle yield results from this process. The line has been placed on the graph to guide the eye.

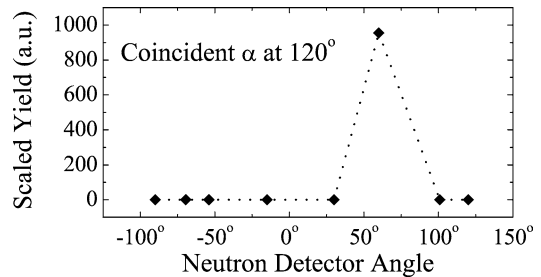


Fig. 5. The number of neutrons coincident with α particles, from the Monte Carlo simulation of projectile breakup under the assumption that the entire α -particle yield results from this process. The detector and experimental parameters from the one-neutron transfer simulations were also used here. The line has been placed on the graph to guide the eye.

the distance of closest approach. Because of the negative Q -value for fragmentation ($Q = -975$ keV), the system loses kinetic energy. In order to simplify the calculation, the remaining kinetic energy was divided among the α particle and the neutrons in proportion to the mass of each particle. The simulated neutrons travel in the direction of the velocity vector of the ${}^6\text{He}$ at the moment of breakup, and therefore are preferentially emitted at about one-half the α -particle angle (Fig. 5). However, their energy is typically about 600 keV, too low to be detected with any efficiency by the neutron detectors used in the present experiment.

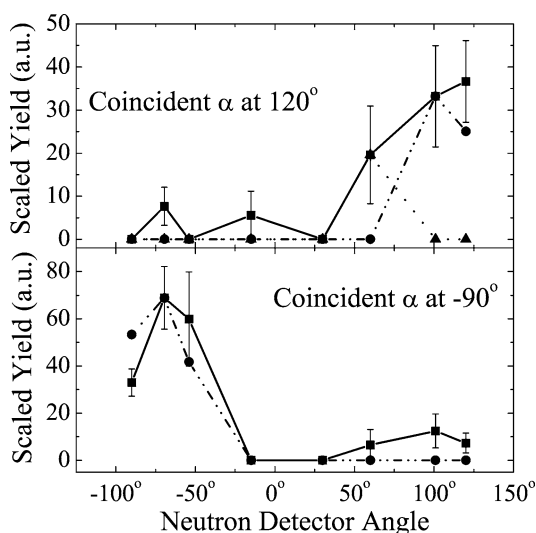


Fig. 6. A comparison of the simulated and observed coincident neutron angular distributions. The square points are the ^{209}Bi -target data. The circular points are the one-neutron-transfer simulations normalized by a factor of 0.225 at 90 degrees and 0.176 at 120 degrees. The triangular points are the projectile-breakup simulation normalized by a factor of 0.02. The lines have been placed on the graph to guide the eye.

(Fig. 5 is shown only for a single detector because there were no neutron detectors at approximately half the angle of the second α detector. The simulation predicted zero counts for all the neutron detectors.)

A comparison of the simulations with experimental data is shown in Fig. 6. It was necessary to scale the ‘predicted’ one-neutron-transfer yield by a factor of 0.225 at 90 degrees and 0.176 at 120 degrees to obtain agreement with experiment. From this we conclude that approximately 20% of the α -particle yield results from one-neutron transfer, and that the relative probability of this process is only weakly dependent on the α -particle angle. There is also some evidence for a very small “direct breakup” yield. However, as noted above, the efficiency for detecting these events is also very small so it is not possible to make any quantitative conclusion regarding the direct-breakup cross section from the present experiment.

Finally, the “evaporation” neutrons following two-neutron transfer should have an isotropic angular distribution. The data (Fig. 6) are consistent, within experimental error, with an isotropic component of intensity about 5 units. Although this seems small, the corresponding integrated yield could account for another

20% to 30% of the α -particle cross section. Moreover, it is important to consider the energy distribution of the “evaporated” neutrons, which we computed with the code PACE2 [12] using the measured Q-value spectrum [8] to determine the initial spin and energy distributions in the compound system after two-neutron transfer. The predicted mean neutron energy is 0.9 MeV, and 63% of the neutrons have energy less than 1 MeV. Since the threshold for neutron detection in this experiment is approximately 1 MeV, most of the α -neutron coincidences from two-neutron transfer would not have been observed. The expected energy distribution of evaporated neutrons after one-neutron transfer (which also leaves the compound system above the neutron emission threshold) has also been computed. In this case the expected mean neutron energy is 0.7 MeV, only 20% of the evaporated neutrons have energy greater than 1 MeV, and 38% of the events result in no neutron at all being emitted.

4. Conclusions

The main conclusion from the above analysis is that the single-neutron transfer process accounts for approximately 20% of the measured, very large α -particle yield in the $^6\text{He} + ^{209}\text{Bi}$ reaction near the Coulomb barrier. The angular dependence of this fractional yield is small and the systematic uncertainty, resulting primarily from the efficiency of the neutron detectors, is estimated to be an additional 10% of the fractional yield (i.e., $\pm 2\%$). It would be very interesting to compare this large one-neutron-transfer yield with calculations including coupling to continuum states, but this calculation has not been carried out. The remaining two processes, two-neutron transfer and direct projectile breakup, presumably share the remaining 80% of the cross section. However, the precise division of the yield between these two modes could not be established. Experiments with a detector having a lower threshold would provide a means to detect the neutrons from these processes with higher efficiency and therefore to determine the individual probabilities based on their characteristic angular distributions. Such experiments are currently in progress using TWINSOL.

Acknowledgements

This work was funded through support from the US National Science Foundation under Grants No. PHY01-40225 (University of Michigan), PHY99-01133 (University of Notre Dame), and PHY01-998061 (Hope College). The construction of the TWINSOL project was funded by the NSF under Academic Research Instrumentation Grant No. PHY95-12199.

References

- [1] P.A. DeYoung, et al., *Phys. Rev. C* 58 (1998) 3442.
- [2] J.J. Kolata, et al., *Phys. Rev. Lett.* 81 (1998) 4580.
- [3] Yu.E. Penionzhovich, *Nucl. Phys. A* 588 (1995) 259c.
- [4] P.A. DeYoung, et al., *Phys. Rev. C* 62 (2000) 047601.
- [5] J.J. Kolata, et al., *Phys. Rev. C* 57 (1998) R6.
- [6] A.S. Fomichev, I. David, Z. Dlouhy, S.M. Lukyanov, Yu.Ts. Oganessian, Yu.E. Penionzhovich, V.P. Perelygin, N.K. Skobelev, O.B. Tarasov, R. Wolski, *Z. Phys. A* 351 (1995) 129.
- [7] M. Trotta, et al., *Phys. Rev. Lett.* 84 (2000) 2342.
- [8] E.F. Aguilera, et al., *Phys. Rev. Lett.* 84 (2000) 5058.
- [9] A. di Pietro, et al., *Europhys. Lett.* 64 (2004) 309;
A. di Pietro, et al., *Phys. Rev. C* 69 (2004) 044613.
- [10] M.Y. Lee, et al., *Nucl. Instrum. Methods Phys. Res. A* 422 (1999) 536.
- [11] S.M. Vincent, et al., *Nucl. Instrum. Methods Phys. Res. A* 491 (2002) 426.
- [12] A. Gavron, *Phys. Rev. C* 21 (1980) 230.